Overtone-induced dissociation and isomerization dynamics of the hydroxymethyl radical (CH2OH and CD2OH). I. A theoretical study

E. Kamarchik, C. Rodrigo, J. M. Bowman, H. Reisler, and A. I. Krylov

Citation: J. Chem. Phys. **136**, 084304 (2012); doi: 10.1063/1.3685891
View online: http://dx.doi.org/10.1063/1.3685891
View Table of Contents: http://jcp.aip.org/resource/1/JCPSA6/v136/i8
Published by the American Institute of Physics.

Overtone-induced dissociation and isomerization dynamics of the hydroxymethyl radical (CH_2OH and CD_2OH). I. A theoretical study

E. Kamarchik,[1,2] C. Rodrigo,[1] J. M. Bowman,[2] H. Reisler,[1] and A. I. Krylov[1,a)]
[1]*Department of Chemistry, University of Southern California, Los Angeles, California 90089-0482, USA*
[2]*Department of Chemistry, Emory University, Atlanta, Georgia 30322-1003, USA*

(Received 1 December 2011; accepted 27 January 2012; published online 24 February 2012)

The dissociation of the hydroxymethyl radical, CH_2OH, and its isotopolog, CD_2OH, following the excitation of high OH stretch overtones is studied by quasi-classical molecular dynamics calculations using a global potential energy surface (PES) fitted to *ab initio* calculations. The PES includes CH_2OH and CH_3O minima, dissociation products, and all relevant barriers. Its analysis shows that the transition states for OH bond fission and isomerization are both very close in energy to the excited vibrational levels reached in recent experiments and involve significant geometry changes relative to the CH_2OH equilibrium structure. The energies of key stationary points are refined using high-level electronic structure calculations. Vibrational energies and wavefunctions are computed by coupled anharmonic vibrational calculations. They show that high OH-stretch overtones are mixed with other modes. Consequently, trajectory calculations carried out at energies about $\sim$3000 cm^{-1} above the barriers reveal that despite initial excitation of the OH stretch, the direct OH bond fission is relatively slow (10 ps) and a considerable fraction of the radicals undergoes isomerization to the methoxy radical. The computed dissociation energies are: $D_0(CH_2OH \rightarrow CH_2O + H) = 10\,188$ cm^{-1}, $D_0(CD_2OH \rightarrow CD_2O + H) = 10\,167$ cm^{-1}, $D_0(CD_2OH \rightarrow CHDO + D) = 10\,787$ cm^{-1}. All are in excellent agreement with the experimental results. For CH_2OH, the barriers for the direct OH bond fission and isomerization are: 14 205 and 13 839 cm^{-1}, respectively. © *2012 American Institute of Physics*. [http://dx.doi.org/10.1063/1.3685891]

I. INTRODUCTION

The chemistry of hydroxyalkyl radicals is important in atmospheric and combustion environments. The prototypical hydroxymethyl radical, CH_2OH, is a significant product in the reaction of $O(^1D)$ with methane,[1] while reactions of halogens with methanol[2] yield predominantly CH_2OH. Hydroxymethyl radicals or their structural isomers, the methoxy radicals, are implicated as intermediates in the $O + CH_3$ and $CH + H_2O$ reactions.[3–6]

Previous experimental and theoretical work on the photophysics and photochemistry of the hydroxymethyl radical focused on its excited Rydberg electronic states and the involvement of conical intersections.[7–10] Vibrational excitation and predissociation of CH_2OH in the ground electronic state has received much less attention because of experimental difficulties. Gas-phase spectroscopic studies of vibrational levels such as the symmetric and antisymmetric CH stretch fundamental vibrations of CH_2OH, as well as excitation of 1–4 quanta of the OH stretch (ν_1 mode) were reported previously.[11–13]

Perhaps the most intriguing result of the previous studies was the observation of overtone-induced vibrational predissociation of CH_2OH upon excitation of the $4\nu_1$ vibrational level.[13] In these studies, the excited OH bond coincided with the bond that was broken. In other cases of overtone-initiated excitation of OH-containing molecules,[14] the broken bond was not excited directly and; therefore, the local oscillator character of the vibration was preserved even above the dissociation threshold. Nevertheless, the existence of a barrier in $CH_2OH \rightarrow CH_2O + H$ reaction[3,15,16] apparently renders sufficient local-mode character to the OH vibration to enable high overtone excitation. The production of H atoms upon excitation near the estimated $4\nu_1 \leftarrow 0$ transition was observed with the action spectrum showing a partially resolved rotational structure. In similar studies of CD_2OH,[13] only H fragments were observed, indicating that isomerization to CHD_2O was at best a minor channel, despite the fact that the available calculations[3,15] all placed the barrier for isomerization to methoxy lower than the barrier for OH bond breaking.

As described previously,[10,15] the minimum energy structure of CH_2OH is non-planar and non-symmetric (C_1) with unequal CH bond lengths. However, there are several non-superimposable conformers that can interconvert over small barriers by inversion at the carbon center or internal rotation about the C–O bond (see Fig. 1 of Ref. 15). The barrier to inversion of the CH_2 group with respect to C_s symmetry is very small and lies below the zero-point energy, and thus the equilibrium structure of the radical spans several conformers.[10,11,15,17] In fact, Johnson and Hudgens[11] concluded that the electronic ground state behaves as A'' (C_s symmetry) with respect to electronic spectroscopy. Nevertheless, as pointed out before,[9,10,15,17] the ground electronic state for the C_1 minimum structure is of A symmetry for which mixing of σ, π, n molecular orbitals (MOs, of a' and a''

a)Author to whom correspondence should be addressed. Electronic mail: krylov@usc.edu.

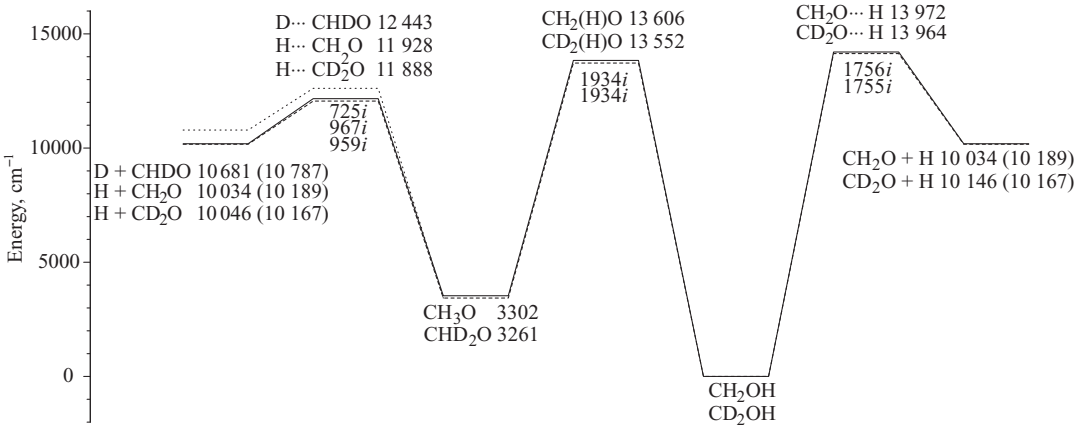

FIG. 1. Energy diagram for ground electronic state dissociation and isomerization of hydroxymethyl radical. All energies are relative to CH_2OH (CD_2OH) vibrational ground state and calculated at RCCSD(T)/CBS level of theory using RCCSD(T)/AVTZ harmonic zero-point energies. For a quantitative comparison with the most recent experimental measurements of dissociation energies the ZPEs of CH_2OH (CD_2OH) and its dissociation products are calculated also using VSCF/VCI. These values are given in parentheses. Corresponding imaginary frequencies are indicated below the barriers. Note the lower barrier for dissociation of CH_3O relative to CH_2OH, and the comparable barriers for OH bond fission and isomerization in CH_2OH.

symmetry in C_s) is allowed. Bruna and Grein calculated the orbital energies of CH_2OH at its minimum energy C_1 structure as well as at the two structures of C_s symmetry (called inversion and rotation).[10] In addition, they reported vertical excitation energies to Rydberg and valence states for these three structures. Yarkony identified conical intersections between the lowest lying Rydberg state, 3s, and the ground electronic state.[9] The previous theoretical studies did not focus on the relative heights of the dissociation and isomerization barriers, which are crucial to the interpretation of the overtone-induced dissociation results.

The goal of the present study is to examine the dissociation dynamics of CH_2OH in the ground electronic state with special emphasis on the role of $CH_2OH \rightarrow CH_3O$ isomerization. We constructed a global potential energy surface (PES) for the $CH_2OH \leftrightarrow CH_3O$ system that spans configurations from the minima of the two isomers to slightly above the dissociation and isomerization barriers. The important configurations and energies for this PES are shown in Figs. 1 and 2. CH_2OH is more stable than CH_3O by $\sim$3300 cm^{-1}. CH_3O requires $\sim$12 000 cm^{-1} relative to the CH_2OH minimum to surmount the barrier to H + CH_2O, while the barrier for CH_2OH decomposition is $\sim$14 000 cm^{-1}, very close in energy to the isomerization barrier (now placed at $\sim$13 600 cm^{-1}) and the employed excitation in the experiments ($\sim$13 600–13 660 cm^{-1}). Whereas the energetically favored pathway for CH_2OH appears to be isomerization, excitation of the OH stretch overtone would not appear to be a mode that promotes this isomerization. Thus, not only the relative barrier heights are of crucial importance, but also the couplings of the OH stretch to other modes at these high energies.

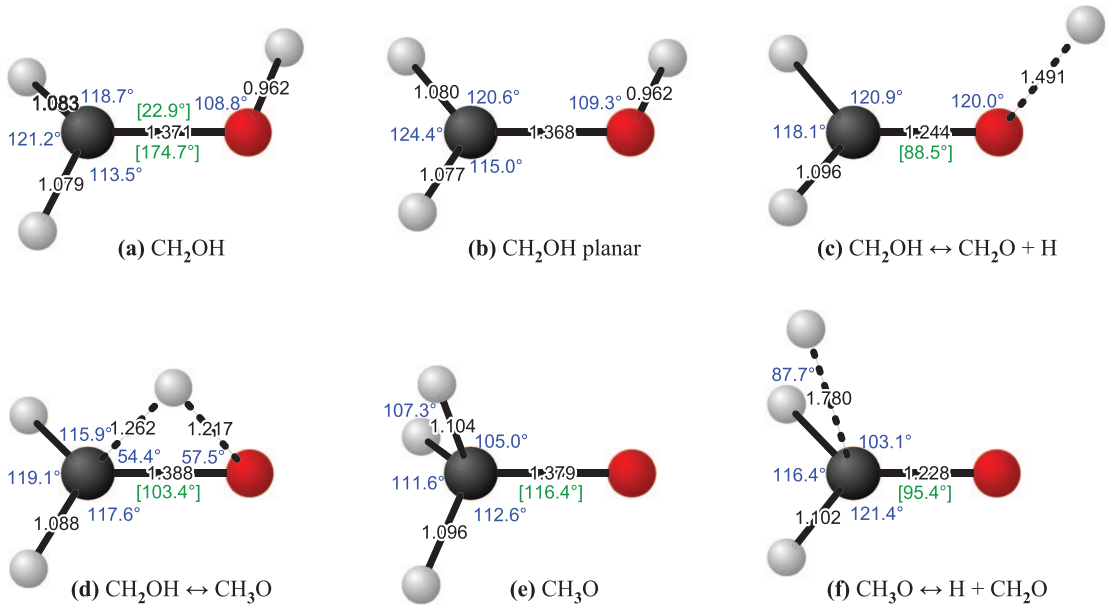

FIG. 2. RCCSD(T)/AVTZ geometries for relevant stationary points of the CH_2OH PES. All structures, except the CH_2OH minimum (a), have C_s symmetry. Bond lengths are in angstroms, dihedral angles are shown in square brackets. CH_2O parameters: $r_{CO} = 1.208$ Å, $r_{CH} = 1.102$ Å, $\angle COH = 121.7°$.

From a theoretical perspective, quantitative studies of the $CH_2OH \leftrightarrow CH_3O$ system near and above the dissociation threshold are challenging for several reasons: (1) accurate calculations of heights and shapes of dissociation and isomerization barriers are required; (2) a global PES that includes all conformers is needed to explore all the feasible dissociation routes; (3) calculating frequencies and couplings of high vibrational states is a daunting task, in particular when the levels are coupled to dissociative continua; (4) the ground state has a conical intersection with the $A'(3s)$ state (this should be of negligible consequence for the present study); and (5) the necessary use of classical dynamics calculations means that the absence of tunneling, and zero-point energy must be acknowledged.

This article reports barrier heights, relevant geometries, dissociation energies, vibrational levels, and rotational constants for CH_2OH and CD_2OH. It also includes results of quasi-classical dynamics simulations that demonstrate both direct OH fission and isomerization pathways. In the paper following this one (Paper II, Ref. 18), new experimental results using velocity map imaging are presented, which give evidence for the participation of direct OH bond fission and isomerization in the overtone-induced predissociation of the hydroxymethyl radical.

II. COMPUTATIONAL DETAILS

The present study employs two different electronic structure methods: density functional theory using the range-separated ωB97X functional,[19] and restricted coupled-cluster with singles, doubles, and perturbative triples, RCCSD(T).[20] The ωB97X calculations were carried out using the Q-Chem suite of quantum chemistry programs,[21] while all RCCSD(T) calculations were performed with MOLPRO.[22] The basis sets used are Dunning's augmented correlation-consistent sets of the triple and quadruple zeta quality (aug-cc-pVTZ and aug-cc-pVQZ, referred hereafter as AVTZ and AVQZ).[23]

The PES for this system has two distinct minima (CH_2OH and CH_3O, the former structure exists as two mirror images) and four saddle points (see Figs. 1 and 2). In order to provide the most accurate relevant energetics, geometry optimizations of each stationary point were performed using RCCSD(T)/AVTZ. A single-point RCCSD(T)/AVQZ energy was then obtained at each geometry, and the correlation energy was extrapolated to the complete basis set (CBS) limit using the standard $1/n^3$ formula.[24] Harmonic frequencies were also obtained at each stationary point at the RCCSD(T)/AVTZ level of theory. These data are provided in supplementary material.[25]

In order to characterize the vibrational energies and couplings of CH_2OH (CD_2OH) as well as the dissociation dynamics, two PESs were constructed. Both PESs are based on the representation of the potential energy using permutationally invariant polynomials in Morse variables,[26] $\exp(-r_{ij}/a)$, where r_{ij} is the internuclear distance between atoms i and j, and a is a reference length (typically $\sim$2 bohr). The first PES was designed to address the vibrational problem and so comprised a fit of 48 226 RCCSD(T)/AVTZ energies, which were concentrated mainly around the CH_2OH minimum, but also reached the barriers for isomerization to CH_3O and for dissociation to $CH_2O + H$. The total polynomial order for this PES was limited to six and the overall root-mean-square (RMS) error of the surface was 82 cm^{-1} (37 cm^{-1} RMS and 305 cm^{-1} max. deviation below 14 000 cm^{-1}). A dipole moment surface was also calculated using a subset of 39 999 of these points at the ωB97X/AVTZ level of theory. The second PES comprised a fit of 74 227 RCCSD(T)/AVTZ energies. This set includes all points from the first dataset plus $CH_2O + H$ fragment data, the CH_3O well, and more points in the transition state regions. The total polynomial order for this PES was limited to 7, and the overall RMS error was 217 cm^{-1} (128 cm^{-1} RMS and 467 cm^{-1} max. below 17 000 cm^{-1}). The larger error in the second potential, despite the increase in the dataset and polynomial order, is because it spans both a considerably larger range of possible geometries and much higher energy configurations than in the PES for vibrational structure. Both PESs employ the ezPES interface.[27] For both PESs, points were chosen first by construction of one-, two-, and a few three-dimensional cuts in internal coordinates centered on the minima and saddle points of interest. These were then supplemented with points generated by classical molecular dynamics trajectories in order to ensure full sampling of configuration space.

It should be noted that while the CH_2OH PES minimum has non-planar geometry (Fig. 2(a)), the two mirror-image configurations are connected by a low-energy ($\sim$100 cm^{-1}) C_s saddle point in which all five atoms are coplanar (Fig. 2(b)). This barrier is so low that the ground vibrational state does not exhibit any tunneling splitting, and its wavefunction maximum (as well as vibrationally averaged structure) corresponds to the planar configuration (see supplementry material[25]). Therefore, this planar saddle point was used as the reference configuration in all vibrational calculations.

Vibrational calculations were performed in full dimensionality (nine normal coordinates) using vibrational configuration interaction/vibrational self-consistent field theory (VCI/VSCF) algorithms, which have been described in the literature previously.[28] In systems that are small enough to permit its use, VCI yields highly accurate vibrational energies that account for anharmonicities and interactions among modes. For CH_2OH (CD_2OH) the VCI calculations were limited to the four-mode representation (4-MR) of the potential and included all vibrational angular momentum terms. At the level of 4-MR, the full-dimensional Hamiltonian is used, but the potential is approximated by a sum of functions depending at most on 4 normal coordinates.[29] Thus only VCI basis functions that have different quanta in four or less normal modes have non-zero Hamiltonian matrix elements. All such excitations with $\leq$5 quanta in each in-plane mode and $\leq$7 quanta in each out-of-plane mode, subject to the total restriction that the sum of quanta $\leq$10, were included in the basis set for the VCI expansion. This resulted in a VCI matrix with two blocks of dimensions 46 799 and 40 464 for A' and A'' symmetry representations, respectively. Comparing with results using a smaller basis indicates that the ZPE and fundamental frequencies are well converged at this basis size.

For dynamics simulations of dissociation and isomerization, 10 000 quasi-classical trajectories were initiated using standard normal-mode sampling. In order to avoid problems associated with classical simulations near the tunneling regime, the initial conditions were chosen at higher energy corresponding to five quanta in the OH stretch mode, i.e., $\sim$3000 cm^{-1} above the barriers. The VCI energies were used to prepare classical harmonic oscillator distributions with appropriate energy in each mode ($5\nu_1$ level energy for the OH stretch mode and $h\nu_i/2$ for ZPE in all other modes), then an anharmonic correction method using the actual PES was applied, as described in Ref. 30. Since the excitation is based on the normal modes calculated at the reference configuration, it does not include the changing character of the vibrational motion at higher excitations and thus always corresponds to a pure OH stretch overtone (normal mode), even if the actual vibrational state is highly coupled by anharmonic effects. This is because the normal mode corresponding to the OH stretch looks like a local mode for just the OH oscillator.

III. RESULTS AND DISCUSSION

A. PES, vibrational energies, and key energetics

The geometries of all relevant stationary points are shown in Fig. 2. The corresponding RCCSD(T)/CBS energies and harmonic frequencies for both isotopologs and their dissociation products are given in supplementary material.[25] The *ab initio* optimizations and frequency calculations indicate that the transition states (TS) leading to isomerization ($CH_2OH \rightarrow CH_3O$) and to OH bond fission ($CH_2OH \rightarrow CH_2O + H$) are both tight and have imaginary frequencies of 1934*i* cm^{-1} and 1756*i* cm^{-1}, respectively. Interestingly, both of these structures are pyramidal (with C_s symmetry) and have HCOH torsional angles close to 90°, indicating that to access either TS, significant torsional motion is required. For the OH bond fission channel this motion can be rationalized by consideration of the relevant molecular orbitals, as described below. The significant torsional changes between the equilibrium geometry and the transition state explain partly why even exciting the "correct" coordinate does not lead only to direct dissociation.

For CH_2OH the fundamental frequencies of all the normal modes obtained from the VCI calculations are in good agreement both with the available experimental values and with the previous theoretical results of Marenich and Boggs.[17] In addition, we present the fundamental frequencies for CD_2OH. The experimental data in this case are incomplete and less robust; nevertheless, we expect similar accuracy of calculations as in the CH_2OH case. Both sets of frequencies together with rotational constants for each level are listed in Tables I and II showing excellent agreement with the experimental results.

As the vibrational energy approaches the dissociation and isomerization barrier tops, the normal-mode picture breaks down as a good zero-order approximation, and identification of pure overtones of any particular normal mode becomes impossible. For the OH stretch, however, a single vibrational state carrying a large coefficient of the associated pure overtone basis function can be identified and, with the exception of $4\nu_1$ in CH_2OH, these are what we report. The recent experimental observation (see Paper II, Ref. 18) of two peaks in the $4\nu_1$ region of the CH_2OH spectrum combined with a similar behavior of OH overtones in methanol[32] suggests the existence of an accidental resonance between the OH stretch and the antisymmetric CH stretch at these energies. The VCI

TABLE I. CH_2OH spectroscopic parameters and zero-point energies (in cm^{-1}) from VCI calculations. Vibrational mode descriptions are approximate; the mixed states in CH_2OH are denoted by leading contributions in their VCI wavefunctions.

	Vibrational level	Energy VCI	Rotational constants A_v	B_v	C_v	Energy Expt.	Rotational constants A_v	B_v	C_v
	ZPE	7956	6.457	0.982	0.855	...	...	...	...
ν_1	OH stretch	3662	6.432	0.975	0.847	3675[a]	6.41[a]	0.96[a]	0.88[a]
ν_2	CH antisymmetric stretch	3116	6.345	0.980	0.854	3162[a]	6.41[a]	0.97[a]	0.88[a]
ν_3	CH symmetric stretch	3020	6.408	0.979	0.854	3043[a]	6.48[a]	0.98[a]	0.88[a]
ν_4	CH_2 scissors	1448	6.493	0.980	0.854	(1459[b])	...	...	...
ν_5	HCOH in-phase bend	1336	6.522	0.982	0.854	(1334[b])	...	...	...
ν_6	CO stretch	1171	6.445	0.974	0.848	1176[c]	...	...	...
ν_7	HCOH out-of-phase bend	1032	6.532	0.981	0.855	(1048[b])	...	...	...
ν_8	HCOH in-phase torsion	468	6.571	0.982	0.857	(420[b])	...	...	...
ν_9	HCOH out-of-phase torsion	244	6.399	0.981	0.859	234[c]	...	...	...
$2\nu_1$		7171	6.288	0.978	0.850	7158[a]	6.39[a]	0.97[a]	0.88[a]
$3\nu_1$		10 514	6.170	0.977	0.845	10 484[d]	6.30[d]	1.00[d]	0.88[d]
$4\nu_1$	$\|1^4\rangle + \|1^3 2^1\rangle$	13 666	6.052	0.981	0.844	13 597[e]	6.1[e]	0.96[e]	0.84[e]
	$\|1^3 2^1\rangle - \|1^4\rangle$	13 767	6.074	0.977	0.843	13 656[e]	6.1[e]	1.00[e]	0.82[e]

[a]From Ref. 12.
[b]From argon matrix study, Ref. 31.
[c]From Ref. 11.
[d]From Ref. 13.
[e]From Ref. 18.

TABLE II. CD_2OH spectroscopic parameters and zero-point energies (in cm^{-1}) from VCI calculations.

	Vibrational level	Energy VCI	Rotational constants A_v	B_v	C_v	Energy Expt.
	ZPE	6747	3.785	0.842	0.692	...
ν_1	OH stretch	3677	3.745	0.841	0.690	(3650[a])
ν_2	CH antisymmetric stretch	2362	3.725	0.840	0.690	...
ν_3	CH symmetric stretch	2198	3.774	0.838	0.688	...
ν_4	CH_2 scissors	1283	3.798	0.839	0.690	...
ν_5	HCOH in-phase bend	1013	3.799	0.842	0.691	1019[b]
ν_6	CO stretch	1201	3.798	0.836	0.689	1208[b]
ν_7	HCOH out-of-phase bend	830	3.812	0.843	0.692	(842[a])
ν_8	HCOH in-phase torsion	461	3.826	0.842	0.693	347[b]
ν_9	HCOH out-of-phase torsion	160	3.765	0.841	0.696	221[b]
$2\nu_1$		7191	3.713	0.839	0.687	...
$3\nu_1$		10 535	3.667	0.841	0.685	...
$4\nu_1$		13 747	3.606	0.841	0.684	13 617[c]

[a]From argon matrix study, Ref. 31.
[b]From Ref. 11.
[c]From Ref. 18.

calculation does indeed indicate such a splitting, as shown in Table I. The absence of two peaks in the corresponding spectrum of CD_2OH in both experiment and calculations supports this interpretation.

Combining the RCCSD(T)/CBS single point energies with the zero-point corrections obtained from VCI allows us to compute accurate dissociation energies (D_0), and these are listed in parentheses in Fig. 1. As will be shown in Paper II,[18] the theoretical values for the $CH_2OH \rightarrow CH_2O + H$, $CD_2OH \rightarrow CD_2O + H$, and $CD_2OH \rightarrow CHDO + D$ channels are in excellent agreement with the experimental ones. The CH_2OH dissociation energy is also in excellent agreement with the calculations of Ref. 17. The other relative energies relevant to the $CH_2OH \leftrightarrow CH_3O$ system that are shown in Fig. 1 are based on harmonic ZPE values; however, we anticipate that they are within about 100 cm^{-1} of the anharmonic results, based on comparisons of the VCI values with D_0 values obtained using a similar harmonic approximation.

B. Dynamical calculations

We also carried out quasi-classical molecular dynamics calculations as described above. When the trajectories were initiated using five quanta in the OH stretch normal mode (16 750 cm^{-1}), a branching between isomerization and OH bond fission of ∽20:80% was obtained. While such simulation does not precisely reproduce the experimental conditions in Paper II,[18] i.e., excitation of $4\nu_1$, it provides a reasonable (in both cases the energy is deposited primarily into the OH stretch coordinate) and feasible-to-calculate ($4\nu_1$ is just at the threshold for these processes and so trajectories using that excitation are both inordinately long and require some approximate treatment of tunneling) estimate of the competition between isomerization and OH bond fission.

As discussed above, the change in geometry of the two TSs relative to the initial configuration requires significant torsional motion of the initially prepared state prior to isomerization or dissociation, and so the trajectories live for an average of ∼10 ps before either event. Dissociation following isomerization occurs fairly rapidly (∼1 ps) due to the much lower barrier for $CH_3O \rightarrow H + CH_2O$ reaction (see Fig. 1). Trajectories initiated using approximate microcanonical sampling[30] above the CH_2OH minimum at the same energy yielded a branching ratio more heavily weighted towards isomerization, ∽60:40 %. This result differs from the one using normal-mode sampling and is farther from the experimental results (see Paper II) indicating that mode-specificity plays a role in the branching. No significant isotope effect was observed in the simulations, with CD_2OH showing branching ratios very similar to CH_2OH in either case. Although there is zero-point adiabatic energy difference of ∼550 cm^{-1} between the dissociation barriers of $CHD_2O \rightarrow CD_2O + H$ and $CHD_2O \rightarrow CHDO + D$, the classical trajectories are likely more sensitive to the potential energy barrier, which is the same in both cases. Sample trajectories illustrative of OH bond fission and isomerization are included in supplementary material.[25]

C. Mechanism of dissociation and isomerization

The theoretical results presented above allow us to propose a mechanism for the production of H and formaldehyde by OH bond fission and via isomerization. Previous work[3,15,33,34] examined the role of isomerization starting from the methoxy radical, and both experiment and theory concluded that isomerization to CH_2OH is unlikely because the barrier for isomerization is significantly higher than the CH_3O dissociation barrier (see Fig. 1). Starting from CH_2OH, however, the barrier to isomerization is slightly lower than that for direct OH bond fission and, as we report here, upon high OH-stretch overtone excitation a minor but significant fraction of the dissociation events proceed through isomerization, in agreement with the experimental results presented in Paper II.

Naively, we may assume that by exciting a vibration that is nominally an OH stretch overtone, energy would be deposited in the coordinate that leads to direct OH bond fission. However, the calculations reveal a more complicated scenario. Vibrational states that have leading coefficients of ν_1 overtones have significant coefficients of other zero-order states and cannot be described as pure OH stretch excitation. Trajectories initiated from the ground state configuration with five quanta in the OH stretch, as described above, require several picoseconds to dissociate even when the available energy exceeds the barrier heights by nearly 3000 cm^{-1}; i.e., they spend considerable time in the bound region of the PES before dissociation.

In addition, the geometries in the TS regions are very different from the equilibrium structure (see Fig. 2). In particular, a large out-of-plane rotation of the OH group is required to attain the geometries of the saddle points. To gain insight, it is instructive to examine more closely the shape of the PES near the TS leading to OH bond fission as a function of the dihedral angle. Figure 3 shows a two-dimensional contour plot of the potential energy as a function of the O–H distance

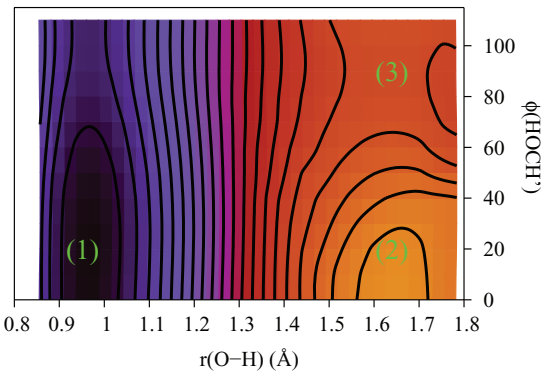

FIG. 3. Contour plot showing the potential energy as a function of the OH bond length and the HOCH' dihedral angle (that equals 22° at the equilibrium geometry, (1)) with all other degrees of freedom relaxed. Dissociation without relaxation of the indicated torsional angle, (2), results in a barrier almost 4000 cm^{-1} above the saddle point, (3). Energy increases from blue to red and orange, interval between countor lines is 1000 cm^{-1}.

and the HCOH' dihedral angle (the dihedral angle connecting hydrogens which are *cis* to each other at the PES minimum), with all other degrees of freedom relaxed.

As described above, in order to reach the TS for OH bond fission, (3), the HCOH' angle needs to change from about 22° to almost 90°. Stretching the OH bond without allowing the dihedral angle to relax, (2), leads to energy higher by nearly 4000 cm^{-1} than the saddle point. Changing the torsional angle at short OH distances (i.e., around equilibrium) results in an energy penalty, whereas the PES is almost flat (along the torsional coordinate) when the OH bond is stretched to 1.2–1.3 Å.

Further insight can be gained by examining the relevant MOs. Figure 4 shows frontier MOs at the three key geometries: the CH_2OH minimum, (1), a structure with the stretched O–H bond and the HCOH' angle fixed, (2), and at the TS, (3). As noted by Bruna and Grein,[10] the doubly occupied orbitals of CH_2OH bear close resemblance to the formaldehyde's MOs; however, the lower (C_1) symmetry of the former enables orbital mixing, especially at distorted geometries.

Indeed, at all three geometries, there is a similarity between the CH_2OH MOs and those of formaldehyde, i.e., HOMO-2 and HOMO-1 of CH_2OH resemble the π and in-plane lone pair, lp(O), orbitals of CH_2O. At the equilibrium geometry, HOMO-1 has OH bonding character revealing that the OH bond is derived from in-phase overlap between in-plane lp(O) and 1s(H). The corresponding anti-bonding, σ^*_{OH}, orbital is higher in energy, and the unpaired electron resides on the lower-energy π^*_{CO} orbital, which weakens the CO bond relative to formaldehyde. Stretching the OH bond results in a change in the SOMO character—it becomes σ^*_{OH}. Overall, stretching the OH bond destabilizes the bonding σ_{OH} orbital and stabilizes σ^*_{OH}, and since the former is doubly occupied and the latter is singly occupied, the overall effect is energetically unfavorable. By increasing the HCOH' angle, as in (3), the overlap between 1s(H) and lp(O) is reduced, and the SOMO and HOMO-1 become non-bonding with respect to the OH interaction (i.e., they become almost pure 1s(H) and lp(O)), which reduces the energy penalty for bond stretching. The effect of the torsion on orbital energies (i.e., stabilization of π^* and destabilization of σ_{OH}) has been noted by Bruna and Grein.[10]

Based on the above analysis we can understand why a TS with a stretched OH bond and a twisted HCOH' angle is lower in energy than a structure that has the same OH bond length but a HCOH' angle frozen at its equilibrium value. Note also that the shape of the SOMO at the TS is similar to the product's orbital (late TS).

Alternatively, the coupling between the OH stretch and the HCOH' angle can be rationalized by looking at the dissociation reaction in reverse, i.e., adding H atom to CH_2O. As the orbital shapes in Fig. 4 suggest, H should interact with the

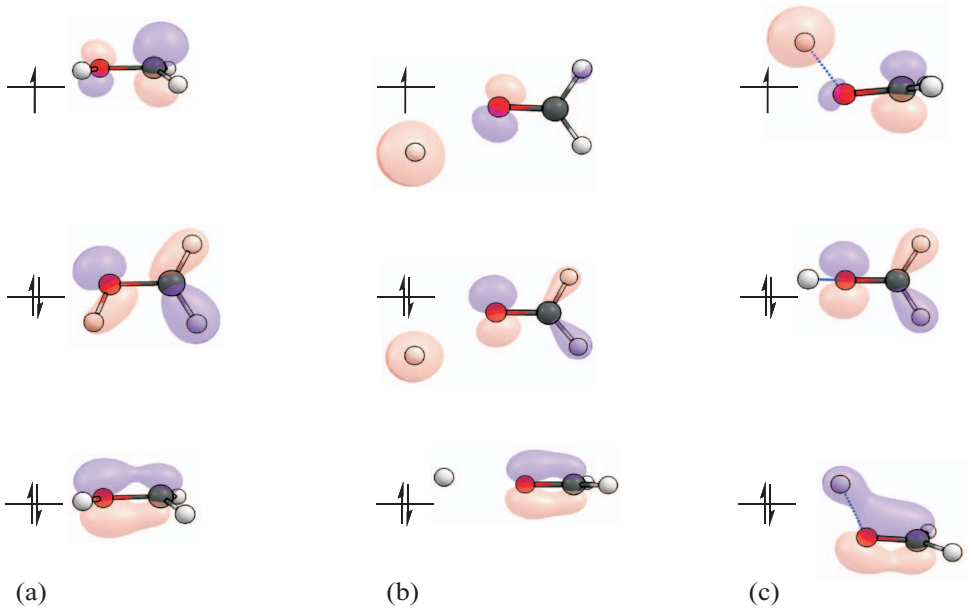

FIG. 4. Frontier MOs (SOMO, HOMO-1, and HOMO-2) at the selected geometries of Fig. 3: equilibrium (a), a structure with the stretched OH bond and the HOCH' angle fixed at the equilibrium value (b), and the TS (c).

π^* orbital and hence approach CH_2O from above or below the plane of the molecule.[16]

The change in the SOMO character (from π^*_{CO} to σ^*_{CO}) upon OH bond stretching is accompanied by a change in wavefunction symmetry (from A'' to A' at planar geometry) that, within the framework of the Woodward-Hoffman rules, would imply the existence of a barrier. We note, however, that in a complex polyatomic system such as CH_2OH orbital correlation diagrams are rather qualitative and do not always represent interactions of many-electron electronic states. This was noted already by Bruna and Grein who discussed the molecular orbitals of ground state CH_2OH in geometries of C_1, A'', and A' symmetries. According to Fig. 3 the change in wavefunction symmetry occurs relatively far from the barrier, at fairly short OH distances, and there is no complementary low-lying valence excited state of π^*_{CO} character that diabatically correlates (at large OH distances) with the ground-state wavefunction (although the energy of the valence $\sigma_{OH} \rightarrow \pi^*$ state is considerably lowered along the OH torsion[10]). The conical intersection of the adiabatic ground-state PES and the Rydberg (3*s*) state occurs at OH distances that are close to their values at the TS (1.35–1.45 Å, see Ref. 9). Treating the couplings among the ground and excited states near the barrier to OH fission is beyond the scope of this paper.

IV. CONCLUSIONS

Global PESs for CH_2OH and CD_2OH were constructed that includes all relevant barriers and dissociation channels. Vibrational levels were calculated for all fundamentals and for ν_1 overtones up to $\sim$14 000 cm^{-1}, and they agree well with the experimental values. Similar good agreement with experiment is obtained for rotational constants and dissociation energies. The electronic structure calculations show that large geometrical changes are required to reach the TSs for OH bond fission and isomerization from the CH_2OH ground vibrational state. In particular, large torsional motion is required to reach the TS for OH bond fission from the ground state minimum. Attempting to remove the hydrogen atom without an accompanying torsional motion results in a barrier nearly 4000 cm^{-1} higher than the dissociation saddle point. In order to reduce the energy penalty for stretching the OH bond, the H atom must be nearly perpendicular to the plane of the formaldehyde fragment. This requires that OH undergoes a large torsional motion with respect to the minimum of ground state CH_2OH, which is nearly planar.

Quasi-classical molecular dynamics calculations demonstrate that radicals excited to $5\nu_1$ are trapped between two barriers of fairly similar heights and shapes and live for several picoseconds even at energies $\sim$3000 cm^{-1} above the dissociation barrier. Dissociation to $H + CH_2O$ can proceed by direct OH bond fission and also via isomerization followed by dissociation. The branching between the two pathways depends on the mode of vibrational excitation. These conclusions are in qualitative agreement with the experimental results described in Paper II.

In conclusion, the $CH_2OH \leftrightarrow CH_3O$ dissociative system has proven to be amenable to both detailed experiments[18] on the dynamics and high-level electronic and vibrational analysis. Most of the previous experimental and theoretical work has dealt with initial excitation of CH_3O for which isomerization is unlikely by energetic considerations. Our work is the first detailed study of vibrational excitation and dissociation of CH_2OH including the role of isomerization. We hope in the future to extend the theoretical studies to investigate the dissociation in the tunneling regime, the role of symmetry and non-adiabatic interactions in the dissociation, and the detailed vibrational and dissociation dynamics in the $CH_2OH \leftrightarrow CH_3O$ system.

ACKNOWLEDGMENTS

This work was conducted under the auspices of the iOpenShell Center for Computational Studies of Electronic Structure and Spectroscopy of Open-Shell and Electronically Excited Species supported by the National Science Foundation through the CRIF:CRF CHE-0625419-0624602-0625237 grant. A.I.K., J.M.B., and H.R. also acknowledge support of the Department of Energy (DE-FG02-05ER15685, DE-FG02-97ER14782, and DE-FG02-05ER15629, respectively). We acknowledge discussions with Mikhail Ryazanov and thank him for sharing his experimental results and his help with article preparation.

[1] J. J. Lin, S. Harich, Y. T. Lee, and X. Yang, J. Chem. Phys. **110**, 10821 (1999); J. J. Lin, J. Shu, Y. T. Lee, and X. Yang, *ibid.* **113**, 5287 (2000).
[2] S. Dóbé, T. Bérces, T. Turányi, F. Márta, J. Grussdorf, F. Temps, and H. Gg. Wagner, J. Phys. Chem. **100**, 19864 (1996); M. Ahmed, D. S. Peterka, and A. G. Suits, Phys. Chem. Chem. Phys. **2**, 861 (2000); S. Rudić, C. Murray, D. Ascenzi, H. Anderson, J. N. Harvey, and A. J. Orr-Ewing, J. Chem. Phys. **117**, 5692 (2002).
[3] T. P. Marcy, R. R. Díaz, D. Heard, S. R. Leone, L. B. Harding, and S. J. Klippenstein, J. Phys. Chem. A **105**, 8361 (2001).
[4] P. W. Seakins and S. R. Leone, J. Phys. Chem. **96**, 4478 (1992); W. Hack, M. Hold, K. Hoyermann, J. Wehmeyer, and T. Zeuch, Phys. Chem. Chem. Phys. **7**, 1977 (2005).
[5] J. Lindner, R. A. Loomis, J. J. Klaassen, and S. R. Leone, J. Chem. Phys. **108**, 1944 (1998); C. Fockenberg, G. E. Hall, J. Preses, T. J. Sears, and J. T. Muckerman, J. Phys. Chem. A **103**, 5722 (1999); V. D. Knyazev, *ibid.* **106**, 8741 (2002); N. Balucani, F. Leonori, A. Bergeat, R. Petrucci, and P. Casavecchia, Phys. Chem. Chem. Phys. **13**, 8322 (2011).
[6] A. Bergeat, S. Moisan, R. Méreau, and J.-C. Loison, Chem. Phys. Lett. **480**, 21 (2009).
[7] L. Feng, A. V. Demyanenko, and H. Reisler, J. Chem. Phys. **120**, 6524 (2004).
[8] V. Aristov, D. Conroy, and H. Reisler, Chem. Phys. Lett. **318**, 393 (2000); D. Conroy, V. Aristov, L. Feng, and H. Reisler, J. Phys. Chem. A **104**, 10288 (2000); L. Feng, X. Huang, and H. Reisler, J. Chem. Phys. **117**, 4820 (2002); L. Feng, A. V. Demyanenko, and H. Reisler, *ibid.* **118**, 9623 (2003); L. Feng and H. Reisler, J. Phys. Chem. A **108**, 9847 (2004).
[9] B. C. Hoffman and D. R. Yarkony, J. Chem. Phys. **116**, 8300 (2002); D. R. Yarkony, *ibid.* **122**, 084316 (2005).
[10] P. J. Bruna and F. Grein, J. Phys. Chem. A **102**, 3141 (1998).
[11] R. D. Johnson III and J. W. Hudgens, J. Phys. Chem. **100**, 19874 (1996).
[12] L. Feng, J. Wei, and H. Reisler, J. Phys. Chem. A **108**, 7903 (2004).
[13] J. Wei, B. Karpichev, and H. Reisler, J. Chem. Phys. **125**, 034303 (2006).
[14] D. W. Chandler, W. E. Farneth, and R. N. Zare, J. Chem. Phys. **77**, 4447 (1982); M.-C. Chuang, J. E. Baggott, D. W. Chandler, W. E. Farneth, and R. N. Zare, Faraday Discuss. Chem. Soc. **75**, 301 (1983); X. Luo, P. R. Fleming, T. A. Seckel, and T. R. Rizzo, J. Chem. Phys. **93**, 9194 (1990); D. Luckhaus, J. L. Scott, and F. F. Crim, *ibid.* **110**, 1533 (1999); B. Kuhn and T. R. Rizzo, *ibid.* **112**, 7461 (2000); F. Reiche, B. Abel, R. D. Beck, and T. R. Rizzo, *ibid.* **112**, 8885 (2000).
[15] S. Saebø, L. Radom, and H. F. Schaefer III, J. Chem. Phys. **78**, 845 (1983).
[16] C. Sosa and H. B. Schlegel, Int. J. Quantum. Chem. **XXIX**, 1001 (1986).

[17]A. V. Marenich and J. E. Boggs, J. Chem. Phys. **119**, 10105 (2003).
[18]M. Ryazanov, C. Rodrigo, and H. Reisler, J. Chem. Phys. **136**, 084305 (2012).
[19]J.-D. Chai and M. Head-Gordon, J. Chem. Phys. **128**, 084106 (2008).
[20]P. J. Knowels, C. Hampel, and H. J. Werner, J. Chem. Phys. **99**, 5219 (1993).
[21]Y. Shao, L. F. Molnar, Y. Jung, J. Kussmann, C. Ochsenfeld, S. Brown, A. T.B. Gilbert, L. V. Slipchenko, S. V. Levchenko, D. P. O'Neil, R. A. Distasio, Jr., R. C. Lochan, T. Wang, G. J. O. Beran, N. A. Besley, J. M. Herbert, C. Y. Lin, T. Van Voorhis, S. H. Chien, A. Sodt, R. P. Steele, V. A. Rassolov, P. Maslen, P. P. Korambath, R. D. Adamson, B. Austin, J. Baker, E. F. C. Bird, H. Daschel, R. J. Doerksen, A. Drew, B. D. Dunietz, A. D. Dutoi, T. R. Furlani, S. R. Gwaltney, A. Heyden, S. Hirata, C.-P. Hsu, G. S. Kedziora, R. Z. Khalliulin, P. Klunziger, A. M. Lee, W. Z. Liang, I. Lotan, N. Nair, B. Peters, E. I. Proynov, P. A. Pieniazek, Y. M. Rhee, J. Ritchie, E. Rosta, C. D. Sherrill, A. C. Simmonett, J. E. Subotnik, H. L. Woodcock III, W. Zhang, A. T. Bell, A. K. Chakraborty, D. M. Chipman, F. J. Keil, A. Warshel, W. J. Herhe, H. F. Schaefer III, J. Kong, A. I. Krylov, P. M. W. Gill, and M. Head-Gordon, Phys. Chem. Chem. Phys. **8**, 3172 (2006).
[22]H.-J. Werner, P. J. Knowles, R. Lindh, F. R. Manby, M. Schütz *et al.*, MOLPRO, version 2006.1, a package of *ab initio* programs, 2006, see http://www.molpro.net.
[23]T. H. Dunning, J. Chem. Phys. **90**, 1007 (1989); R. A. Kendall, T. H. Dunning, and R. J. Harrison, *ibid.* **96**, 6796 (1992).
[24]T. Helgaker, W. Klopper, H. Koch, and J. Noga, J. Chem. Phys. **106**, 9639 (1997).
[25]See supplementary material at http://dx.doi.org/10.1063/1.3685891 for the *ab initio* Cartesian geometries, relevant energies, and density plots of vibrational states, and sample trajectories.
[26]B. J. Braams and J. M. Bowman, Int. Rev. Phys. Chem. **28**, 577 (2009).
[27]E. Kamarchik, B. Braams, A. I. Krylov, and J. M. Bowman, ezPES, see http://iopenshell.usc.edu/downloads/.
[28]J. M. Bowman, J. Chem. Phys. **68**, 608 (1978); J. M. Bowman, T. Carrington, and H.-D. Meyer, Mol. Phys. **106**, 2145 (2008).
[29]S. Carter, S. J. Culik, and J. M. Bowman, J. Chem. Phys. **107**, 10458 (1997).
[30]G. H. Peslherbe, H. Wang, and W. L. Hase, Adv. Chem. Phys. **105**, 171 (1999).
[31]M. E. Jacox, Chem. Phys. **59**, 213 (1981).
[32]O. V. Boyarkin, L. Lubich, R. D. F. Settle, D. S. Perry, and T. R. Rizzo, J. Chem. Phys. **107**, 8409 (1997).
[33]A. Geers, J. Kappert, F. Temps, and J. W. Wiebrecht, J. Chem. Phys. **99**, 2271 (1993); **101**, 3618 (1994); S. Dertinger, A. Geers, J. Kappert, J. W. Wiebrecht, and F. Temps, Faraday Discuss. **102**, 31 (1995).
[34]L. A. Curtiss, L. D. Kock, and J. A. Pople, J. Chem. Phys. **95**, 4040 (1991); S. P. Walch, *ibid.* **98**, 3076 (1993); N. D. K. Petraco, W. D. Allen, and H. F. Schaefer III, *ibid.* **116**, 10229 (2002); T. Taketsugu, N. Tajima, and K. Hirato, *ibid.* **105**, 1933 (1996); T. Yanai, T. Taketsugu, and K. Hirato, *ibid.* **107**, 1137 (1997).